

# Identification of a cell-penetrating peptide domain from human beta-defensin 3 and characterization of its anti-inflammatory activity

Jue Yeon Lee<sup>1,\*</sup>  
Jin Sook Suh<sup>2,\*</sup>  
Jung Min Kim<sup>1</sup>  
Jeong Hwa Kim<sup>1</sup>  
Hyun Jung Park<sup>1</sup>  
Yoon Jeong Park<sup>1,2</sup>  
Chong Pyoung Chung<sup>1</sup>

<sup>1</sup>Central Research Institute, Nano Intelligent Biomedical Engineering Corporation (NIBEC), Chungcheongbuk-do, Republic of Korea; <sup>2</sup>Dental Regenerative Biotechnology, Dental Research Institute, School of Dentistry, Seoul National University, Seoul, Republic of Korea

\*These authors contributed equally to this work

Correspondence: Yoon Jeong Park  
Dental Regenerative Biotechnology,  
School of Dentistry, Seoul National  
University, 101 Daehak-ro, Jongno-gu,  
Seoul 151-749, Republic of Korea  
Tel +82 2 740 8651  
Fax +82 2 744 8732  
Email parkyj@snu.ac.kr

Chong Pyoung Chung  
Central Research Institute, Nano  
Intelligent Biomedical Engineering  
Corporation (NIBEC), Iwol Electricity-  
electronic Agro-industrial Complex,  
116, Bamdi-gil, Iwol-myeon, Jincheon-gun,  
Chungcheongbuk-do 27816, Republic  
of Korea  
Tel +82 43 532 7458  
Fax +82 43 537 1714  
Email ccpperio@snu.ac.kr

**Abstract:** Human beta-defensins (hBDs) are crucial factors of intrinsic immunity that function in the immunologic response to a variety of invading enveloped viruses, bacteria, and fungi. hBDs can cause membrane depolarization and cell lysis due to their highly cationic nature. These molecules participate in antimicrobial defenses and the control of adaptive and innate immunity in every mammalian species and are produced by various cell types. The C-terminal 15-mer peptide within hBD3, designated as hBD3-3, was selected for study due to its cell- and skin-penetrating activity, which can induce anti-inflammatory activity in lipopolysaccharide-treated RAW 264.7 macrophages. hBD3-3 penetrated both the outer membrane of the cells and mouse skin within a short treatment period. Two other peptide fragments showed poorer penetration activity compared to hBD3-3. hBD3-3 inhibited the lipopolysaccharide-induced production of inducible nitric oxide synthase, nitric oxide, and secretory cytokines, such as interleukin-6 and tumor necrosis factor in a concentration-dependent manner. Moreover, hBD3-3 reduced the interstitial infiltration of polymorphonuclear leukocytes in a lung inflammation model. Further investigation also revealed that hBD3-3 downregulated nuclear factor kappa B-dependent inflammation by directly suppressing the degradation of phosphorylated-I $\kappa$ B $\alpha$  and by downregulating active nuclear factor kappa B p65. Our findings indicate that hBD3-3 may be conjugated with drugs of interest to ensure their proper translocation to sites, such as the cytoplasm or nucleus, as hBD3-3 has the ability to be used as a carrier, and suggest a potential approach to effectively treat inflammatory diseases.

**Keywords:** human beta-defensin 3, cell-penetrating peptide, anti-inflammatory activity, lipopolysaccharide, NF- $\kappa$ B canonical pathway

## Introduction

Cationic antimicrobial peptides (AMPs), a class of bioactive peptides that are structurally analogous to cationic cell penetrating peptides, are an essential part of the innate immune system in most living organisms.<sup>1</sup> Indeed, the desire to more effectively treat inflammatory diseases without side effects has spurred medical researchers to contrive new therapies, including novel anti-inflammatory reagents, such as AMPs. These peptides share several features, such as a relatively short length (10–40 amino acids), and a highly positive net charge, which is essential for binding negatively charged extracellular matrix molecules and outer membrane phospholipids to penetrate bacteria. AMPs are capable of eliminating pathogens, such as bacteria, viruses, and fungi, by directly binding their membranes to prevent the colonization of host tissues.<sup>2</sup> AMPs fall into several categories based on their secondary structural features, namely, linear  $\alpha$ -helix structures, extended structures, loop structures, and  $\beta$ -sheet structures, such as human defensins.<sup>3</sup> Among the known defensins,  $\beta$ -defensins (hBDs) possess

intramolecular disulfide bridges between cysteine residues to stabilize their structures. These peptides are thought to serve as the host's first line of defense because of their ability to immediately and precisely recognize and neutralize infecting pathogens. In addition to their antimicrobial activity, hBDs exert a modulatory effect on inflammation and act as chemoattractants for monocytes, lymphocytes, and dendritic cells, suggesting that AMPs play an important role in both innate and adaptive immunity.<sup>4</sup> Although their initial mechanism of action is closely connected with membrane penetration, the exact mechanisms of hBD activity are only beginning to be elucidated.<sup>5,6</sup> Among the identified hBDs, hBD3 is attractive for potential pharmaceutical applications as an antibiotic and as a modulator of inflammation.<sup>5</sup> hBD3 undergoes spontaneous self-oligomerization and shows antibacterial activity against Gram-positive bacteria, and its role in adaptive immune responses is biologically significant compared to hBD1 and hBD2.<sup>7,8</sup>

Although therapeutic applications have been suggested for hBD3, there are some limitations to its use, including its size, the complexity of disulfide pairing, and the attenuated activity due to elevated ionic strength. Many previous studies have evaluated several peptide fragments of hBD3 that differ in their disulfide connectivity, length, cationic charge, and hydrophobicity, and these fragments are tested against various bacteria.<sup>9–11</sup> The antimicrobial activity of hBD3 has been shown to be independent of the order of disulfide pairings and can withstand cysteine residue substitution.<sup>11</sup> A C-terminal hBD3 peptide in which the cysteine residues were replaced with serine was found to show antimicrobial activity against *Escherichia coli*. Alternatively, an N-terminal hBD3 peptide containing cysteine-to-serine substitutions showed anti-microbial activity against *Candida albicans* and *Staphylococcus aureus*.<sup>9</sup>

Nevertheless, the anti-inflammatory activity of peptides derived from hBD3 has yet to be examined. The aim of this study was to investigate a peptide fragment of hBD3 with cell-penetrating activity and demonstrate its

anti-inflammatory effects in vitro and in vivo. Three peptide fragments were synthesized, and their skin- and macrophage-penetrating activities were investigated. A cell-penetrating peptide fragment was selected, and its anti-inflammatory activity was investigated in endotoxin-induced macrophages and an inflammation animal model by quantifying the levels of active NF- $\kappa$ B and cytokines.

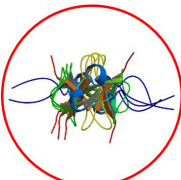
## Materials and methods

### Materials

Dulbecco's Modified Essential Medium (DMEM), Hank's balanced salt solution, trypsin-ethylenediaminetetraacetic acid, fetal bovine serum (FBS), phosphate-buffered solution (PBS), and an antibiotic-antimycotic solution were purchased from Thermo Fisher Scientific (Waltham, MA, USA). Antibodies against NF- $\kappa$ B p65, I $\kappa$ B $\alpha$ , iNOS, and phosphorylated I $\kappa$ B $\alpha$  were purchased from Cell Signaling Technology, Inc. (Beverly, MA, USA), and secondary antibodies were purchased from Santa Cruz Biotechnology, Inc. (Dallas, TX, USA). Other chemicals, including lipopolysaccharide (LPS) and bovine serum albumin, were obtained from Sigma-Aldrich Co. (St Louis, MO, USA).

### Peptide preparation

Automated synthesis of three peptides derived from hBD3 (Figure 1) was carried out on a midi-scale peptide synthesizer (Endeavor 90, AAPP TEC, USA) to yield the C-terminal amide form using standard 9-fluorenylmethoxycarbonyl chemistry. Peptides were purified by preparative reverse-phase high-performance liquid chromatography (Waters, USA), with a Vydac C18 column and 50-minute gradient from 90% to 10% water/acetonitrile containing 0.1% trifluoroacetic acid. The purity of the synthetic peptides was determined by high-performance liquid chromatography analysis or liquid chromatography–mass spectrometry analysis. All purities were >90%. To detect the translocation pathways of the peptides, the synthetic peptides were manually conjugated at the N-terminus with the red dye rhodamine



PDB ID: 1JK6\_A

	Sequence	Theoretical pI	Theoretical MW	Net charge
hBD3-1	GINTLQKYCYCRVRG	9.78	1,670.95	+3
hBD3-2	GRCVLSCLPKEQI	8.06	1,516.84	+1
hBD3-3	GKCSTRGRKCCRRKK	11.02	1,767.17	+8

**Figure 1** The structure of hBD3 and the physical properties of the hBD3 peptide fragments.

**Abbreviations:** hBD3, human beta-defensin 3; MW, molecular weight; pI, isoelectric point; PDB ID, protein data bank identification.

B during synthesis.<sup>12</sup> The purity and efficiency of rhodamine labeling were investigated via high-performance liquid chromatography by monitoring the absorbance at 230 nm and fluorescence at 560 nm.

## Cell culture

The macrophage cell line RAW 264.7, derived from the American Type Culture Collection (ATCC, MD, USA), was cultured in DMEM supplemented with 10% FBS and maintained at 37°C in a humidified atmosphere of 5% CO<sub>2</sub>.

## In vitro cellular internalization

Cells (1×10<sup>4</sup> cells) were seeded overnight on glass slides (Thermo Fisher Scientific). Following a 24-hour incubation to allow cells to attach, the culture media were removed, and 50 μM of rhodamine-labeled peptide was added along with fresh complete media. After treatment for 10 minutes at 37°C in a 5% CO<sub>2</sub> atmosphere, the cells were washed with PBS and incubated with 1 μg/mL 4',6-diamidino-2-phenylindole for 20 minutes at room temperature to stain nuclei. The cells were washed, and the samples were imaged on an Olympus FV-300 confocal laser scanning microscope operated with FLUOVIEW software (Olympus, Tokyo, Japan).

Cells (1×10<sup>6</sup> cells) were seeded on six-well plates in a complete medium. One day later, the cells were preincubated in DMEM without FBS for 1 hour. Then, 50 μM of rhodamine-labeled peptide was added to the cells along with fresh complete media for 30 minutes in a CO<sub>2</sub> incubator and then removed by washing three times with PBS. The cells were harvested using 0.25% trypsin-ethylenediaminetetraacetic acid for 15 minutes, which also helped to remove excess rhodamine-labeled peptides bound to the outer membrane and reduce the occurrence of artifacts.<sup>13</sup> Cellular uptake of the fluorescent peptide was investigated by using flow cytometry (FACSCalibur, Becton Dickinson, CA, USA). Fluorescence emission was detected using a 575/24 nm bandpass filter (FL2) for rhodamine. The data were analyzed from three independent experiments in each group.

## In vivo skin penetration

Athymic nude mice (5 weeks old, male; Japan SLC Inc., Shizuoka, Japan) were freely fed water and rodent food for at least 7 days to acclimate to the Animal Care Facilities of Seoul National University. Animal experiments in this study were conducted in strict accordance with the standard ethical guidelines and were approved by Seoul National University Animal Care and Use Committee (SNU-110610-2). To test which parts of hBD3 were able to

cross the skin, the rhodamine-labeled peptides were dissolved in PBS (100 μg/20 μL) and were then applied to separate locations on the back of a nude mouse. Following a 3-hour treatment, the mice were sacrificed, and their dermal tissues were removed from the dorsal side. The experiments were repeated with triplication in each group. Skin specimens were washed with PBS and embedded in Tissue-Tek® OCT compound (Pelco International, CA, USA). The tissues were sectioned into 8 μm thick slices using a cryocut microtome (Leica, Wetzlar, Germany). The skin delivery of the peptides was visualized by assessing the penetration of the fluorescent dyes by confocal laser scanning microscopy (Olympus FV-300, Osaka, Japan). All optical sections were investigated with the same settings.

## Western blot analysis

Following incubation with the peptides, the cells were washed and detached to collect cell pellets. Cytoplasmic and nuclear fractions were prepared using an extraction kit (NE-PER®; Pierce, IL, USA), according to the manufacturer's instructions. Protein concentrations were determined for all samples by Bradford's method. Proteins in each sample were separated via sodium dodecyl sulfate-polyacrylamide gel electrophoresis using a previously established buffer system.<sup>14</sup> After electrophoresis, the proteins were transferred to nitrocellulose membranes and blocked in 5% nonfat dried milk/Tris-buffered saline containing 0.05% Tween. Primary antibodies against iNOS, phospho-IκBα, IκBα, and NF-κB p65, followed by horseradish peroxidase-conjugated goat anti-mouse or anti-rabbit immunoglobulin G antibodies were applied. Protein-antibody blots were detected using a subtractive reagent, West-Zol (Intron, Seoul, Korea), and captured with Microchemi (DNR Bio-imaging systems, Jerusalem, Israel). The data were analyzed from three independent experiments in each group.

## In vitro quantitative analysis of secreted molecules

NO synthesis was evaluated by analyzing cell supernatants for nitrite using a previously described microplate assay.<sup>15</sup> Each 100 μL aliquot of culture medium was added to an equal volume of Griess-Saltzman reagent, which was prepared from 0.1% (w/v) *N*-(1-naphthyl)-ethylenediamine dihydrochloride and 1% (w/v) sulfanilamide in 2.5% (v/v) H<sub>3</sub>PO<sub>4</sub> and incubated in the dark for 10 minutes at room temperature. Absorbance was measured at 540 nm using a microplate reader to determine the nitrite concentration. NaNO<sub>2</sub> was used as a standard. To investigate the levels of secreted cytokines, the concentrations of TNF-α and IL-6 in the supernatants

after LPS treatment were quantified using an enzyme-linked immunosorbent assay kit (R&D, MN, USA), according to the manufacturer's instructions. The data were analyzed from three independent experiments in each group.

### Cell viability assay

Complete medium containing  $5 \times 10^5$  cells/well was added to 24-well plates and treated with various concentrations of hBD3. After incubation at 37°C, 5% CO<sub>2</sub> for 24 hours to adhere the cells, cell metabolic activity was measured by detecting mitochondrial respiration via the change of the tetrazolium bromide salt into its insoluble formazan. After treatment with peptides for 24 hours, 3-(4,5-dimethylthiazol-2-yl)-2,5-diphenyltetrazolium bromide solution was added to the cells to a final concentration of 0.5 mg/mL. The medium was then removed after incubation for 4 hours at 37°C, and 500 µL of dimethyl sulfoxide was added to dissolve the formazan precipitates. A 200 µL aliquot from each well was then transferred to a 96-well plate, and the absorbance was read at 540 nm on a microplate reader (Bio-Tek, VT, USA). The data were analyzed from three independent experiments in each group.

### Immunofluorescence confocal microscopy

Twenty-four hours after seeding on glass coverslips, RAW 264.7 cells were washed with PBS. Then, cells were fixed immersing the coverslips in 4% neutral paraformaldehyde for 10 minutes, and 0.1% Triton-X100/PBS was added for 5 minutes at room temperature to improve permeability. The cells were blocked with 5% bovine serum albumin for 20 minutes and then incubated with NF-κB p65 antibody (1:100) for 1.5 hours to investigate the nuclear translocation of active NF-κB. Following incubation, the cells were washed with PBS and then stained for 1 hour with a fluorescein isothiocyanate-conjugated donkey anti-rabbit immunoglobulin G antibody (1:100). Nuclei were stained with 4',6-diamidino-2-phenylindole (1:5,000; Thermo Fisher Scientific), and the cells were mounted and analyzed on an Olympus FV-300 confocal laser scanning microscope controlled by FLUOVIEW software (Olympus, Tokyo, Japan). The data were evaluated from three independent experiments in each group.

### Anti-inflammatory effect on induced inflammation of lung tissues

The Institutional Animal Care and Use Committee at the College of Dentistry of Seoul National University approved

all experiments. Male Wistar rats (5–6 weeks old; Japan SLC Inc., Shizuoka, Japan) were allowed to acclimatize to specific pathogen-free conditions for at least 7 days before handling. To develop the induced inflammatory animal model, the rats were treated with intravenous injection of 500 µg of LPS, with or without hBD3-3 dissolved in PBS. At 2 hours after treatment with the peptides, the rats were sacrificed via intramuscular injection with 80 mg/kg ketamine and 8 mg/kg xylazine. The experiments were performed from three independent batches in each group. The lung tissues were dissected, and blood was collected from the inferior vena cava to vacutainer tubes. To investigate sectioned lung tissues, the lungs were inflated with 4% (v/v) neutral buffered formalin for 24 hours and embedded in paraffin using a routine method. Then, 5 µm thick slices prepared using a sharp blade beginning at a position chosen were stained with hematoxylin and eosin to visualize the pathological changes caused by inflammatory responses in the lungs. The histological alterations were quantitatively analyzed as indexes of the severity of neutrophil infiltration at a magnification of 400× on each slide in five animals from each group. Lung injury was observed in a blinded fashion. Samples of plasma fluid were collected from whole blood by centrifugation, snap frozen in liquid nitrogen, and stored at –80°C for cytokine analysis.

### Statistical analysis

All quantitative results were normalized to the mean of each control group and independently repeated at least in triplicate. All values were expressed as the mean ± standard deviation. One-way analysis of variance with triplication was used to compare all study groups with the control group, followed by Fisher's exact test to identify the association between changes. Any *P*-values <0.05 were accepted as statistically significant.

## Results

### Cell and skin penetration by hBD3-3

hBD3 contains 45 amino acids. Three 15-amino-acids peptides (hBD3-1, hBD3-2, hBD3-3) were generated from the hBD3 protein starting at the N-terminus (Figure 1). The hBD3-3 peptide includes eight basic amino acids and features a higher net positive charge than the other peptides. The hBD3-3 sequence shows conserved identities to that of cell-penetrating peptides.<sup>16</sup> Peptide charge, as determined by arginine, lysine, and histidine residues, helps to bind negatively charged cell surface molecules, and arginine, in particular, can trigger the cellular uptake through endocytosis. By far,



the most commonly known CPP is transactivator of transcription, discovered from human immunodeficiency virus-type 1, which delivers various cargo molecules into cells and whose net charge is also determined by arginine.<sup>17,18</sup> We investigated the ability of the three hBD3 peptide fragments to penetrate the outer membrane of cells, as well as mouse skin. The cellular internalization of the three peptides was visualized via confocal microscopy after 10 minutes and 30 minutes of treatment. Figure 2A indicates that cytosolic fluorescence could not be observed for hBD3-1, hBD3-2, or a mismatch peptide of hBD3-3. In contrast, hBD3-3 was significantly internalized by cells, consistent with its positive charge. We quantified peptide internalization via flow cytometry to more accurately evaluate hBD3-3-mediated uptake ability (Figure 2B). The internalization of hBD3-3 was measured based on the mean fluorescent intensity of each sample. The flow cytometry data correlated with confocal microscopy analyses, and the hBD3-3 was detected in the cells both after 10 minutes and 30 minutes of incubation. As shown in Figure 2A and B, the cell-uptake analyses clearly demonstrated that hBD3-3 effectively translocated into cells, including into the cytosol. The potential of hBD3-3 to penetrate the skin of nude mice was monitored via confocal microscopy (Figure 3). Skin loaded with PBS as a mock control exhibited slight autofluorescence. Treatment of the skin with rhodamine-labeled hBD3-1, hBD3-2, or the mismatch peptide resulted in fluorescent staining of the stratum corneum, with only very faint color being observed in the epidermis. However, in skin treated with rhodamine-labeled hBD3-3, we observed strong red fluorescence in the epidermis and weak fluorescence in the dermis (Figure 3). The thickness of the stratum corneum is 20  $\mu\text{m}$ , and that of the epidermis is 100  $\mu\text{m}$ .<sup>19,20</sup> The tissue-penetration activity of hBD3-3 suggested the potential for transdermal application rather than injection to overcome the thicknesses of these tissues. These results were consistent with the *in vitro* cell penetration of hBD3-3.

### Effects of hBD3-3 on nitrite and cytokine production *in vitro*

To test the possibility that hBD3-3 might act as a modulator of inflammation, LPS-treated RAW264.7 cells were used as a model of inflammatory processes. We first measured NO production in RAW 264.7 cells, as this is a characteristic feature of activated macrophages. LPS treatment strongly induced NO production in the cells, and pretreatment with various concentrations of the peptides for 1 hour prior to LPS (1  $\mu\text{g/mL}$ ) stimulation for 18 hours significantly blocked LPS-induced NO production in a dose-dependent manner

(Figure 4A). hBD3-3 inhibited LPS-induced NO production by nearly 50% compared with the negative control. To investigate the involvement of hBD3-3 in iNOS expression, we examined iNOS protein levels in the macrophages following LPS stimulation. The change in iNOS expression following LPS treatment was markedly inhibited by hBD3-3 (Figure 4B and C).

The LPS-stimulated expression of IL-6 and TNF- $\alpha$  was also dramatically suppressed by hBD3-3 in the cells (Figure 4D and E). At 200  $\mu\text{M}$ , the peptide almost completely blocked the expression of LPS-induced proinflammatory cytokines such as TNF- $\alpha$  and IL-6. We also examined the effect of hBD3-3 on cell viability to evaluate its potential use as an anti-inflammatory drug. As shown in Figure 4F, the hBD3-3 had no effect on mouse macrophage viability.

### Effects of hBD3-3 on lung injury and plasma cytokines in inflammation-induced rats

To determine whether hBD3-3 also downregulates inflammatory responses *in vivo*, we first investigated the effects of hBD3-3 on inflammatory signals caused by systemic inoculation with LPS for 2 hours. Among the known inflammatory signal molecules, cytokine in plasma samples were examined as a direct indicator of inflammatory responses *in vivo*. As shown in Figure 5A and B, intravenous treatment with hBD3-3 suppressed the induction of IL-1 $\beta$  and TNF- $\alpha$  in the plasma in a concentration-dependent manner after LPS inoculation. hBD3-3 administration also significantly inhibited the infiltration of polymorphonuclear neutrophils into the interstitial and peribronchial sites of LPS-induced lung injury (Figure 5C). The levels of migrated neutrophils in the lungs were significantly greater in the LPS-treated rats and were markedly reduced in rats treated with hBD3-3 or with an inflammatory inducer alone. However, the negative control and hBD3-3-only-treated groups showed no alteration in neutrophil infiltration (Figure 5D). Taken together, these results clearly suggest that hBD3-3 has the potential to inhibit inflammatory responses without immunogenicity itself both *in vitro* and *in vivo*.

### Effects of hBD3-3 on LPS-stimulated NF- $\kappa\text{B}$ activity

Because the stimulation of NF- $\kappa\text{B}$  activity is critical for iNOS and cytokine expression, the activation of NF- $\kappa\text{B}$  was investigated in cells using Western blotting to assess the effects of hBD3-3 on the early stages of inflammatory

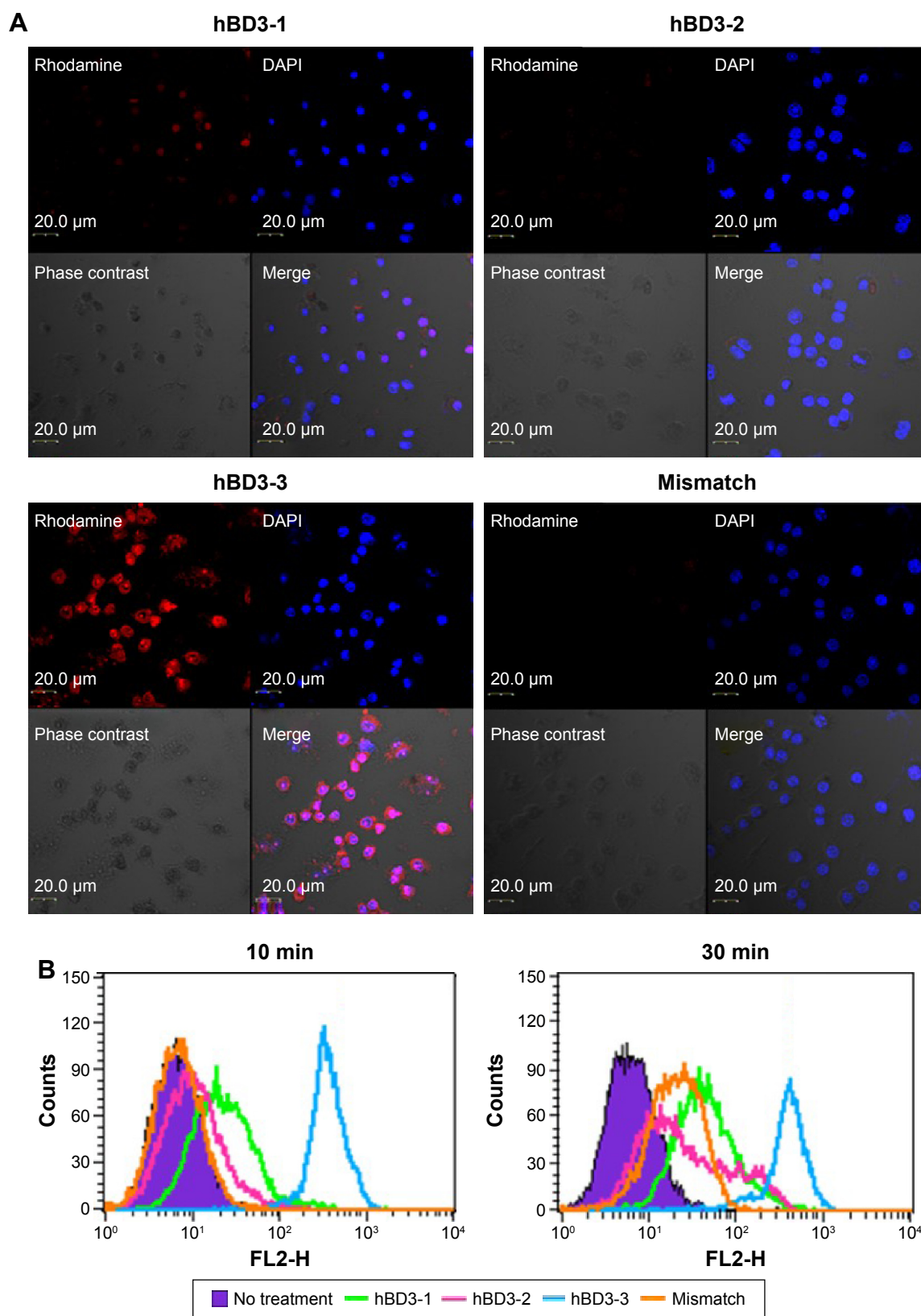


**Figure 2** Intracellular translocation of hBD3-3 in vitro.

**Notes:** (A) Cellular localization of rhodamine-labeled peptide fragments in RAW 264.7 cells. Cells ( $1 \times 10^4$ ) were incubated for 10 minutes in medium containing the rhodamine-labeled peptides (50  $\mu$ M) (original magnification 40 $\times$ ). (B) FACS analysis of cells treated with rhodamine-labeled peptides. Cells ( $1 \times 10^6$ ) were incubated for 10 minutes and 30 minutes in medium containing the rhodamine-labeled peptides (50  $\mu$ M).

**Abbreviations:** hBD3, human beta-defensin 3; FACS, fluorescence-activated cell sorting; DAPI, 4',6-diamidino-2-phenylindole; min, minutes.

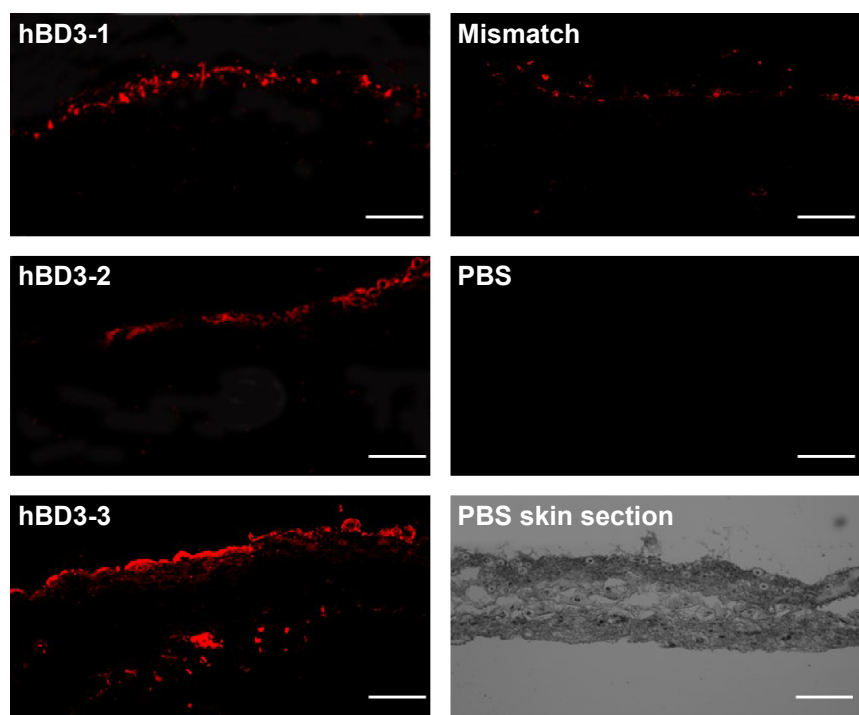


**Figure 3** Skin penetration activity of hBD3-3 in vivo.

**Notes:** Fluorescence microscopy of nude mouse skin sections 3 hours after application of PBS or rhodamine-labeled peptides. Sections were visualized using a rhodamine filter. Scale bar, 200  $\mu$ m.

**Abbreviations:** hBD3, human beta-defensin 3; PBS, phosphate-buffered saline.

responses.<sup>21</sup> Because we found that hBD3-3 markedly blocked LPS-induced iNOS expression, we assessed the effect of hBD3-3 on LPS-stimulated NF- $\kappa$ B activity. Previous studies have demonstrated that I $\kappa$ B kinase can phosphorylate I $\kappa$ B $\alpha$  and I $\kappa$ B $\beta$ , which targets them for ubiquitin–proteasomal degradation. The degradation of I $\kappa$ Bs leads to NF- $\kappa$ B activation, which induces the nuclear translocation of the NF- $\kappa$ B p65 subunit, thereby targeting the promoters of inflammation marker genes and activating the expression of inflammatory factors.<sup>22,23</sup> In these experiments, LPS-stimulated I $\kappa$ B $\alpha$  phosphorylation and degradation were significantly inhibited by pretreatment with hBD3-3 (Figure 6A–C). Moreover, the LPS-induced nuclear translocation of the NF- $\kappa$ B p65 subunit was also completely suppressed upon preincubation with 200  $\mu$ M hBD3-3 (Figure 6D–F).

## Discussion

hBD3, which is 45 amino acids in length, is a cationic peptide with antimicrobial and immunomodulatory activities.<sup>24</sup> The antimicrobial mechanism of hBD3 includes disrupting the negatively charged bacterial membrane by passing through it, causing the leakage of cellular contents and, ultimately, the destruction of the cell.<sup>25,26</sup> hBD3 has been

demonstrated to induce potent mediators of inflammation in keratinocytes<sup>27</sup> and inflammatory cells.<sup>28</sup> Among these cells, macrophages play a critical role in innate immunity in early inflammatory processes and are the main source of proinflammatory mediators, such as NO, iNOS, and COX-2, as well as cytokines, such as IL-6 and IL-1 $\beta$ .<sup>29–31</sup> In addition, mitogen-activated protein kinases and NF- $\kappa$ B have been associated with the overproduction of these inflammatory mediators.<sup>32</sup> In previous studies, proinflammatory cytokines, such as TNF- $\alpha$  and IL-6, were completely blocked by hBD3 in pathogen-induced macrophages isolated from human bone marrow both in vitro and in vivo<sup>33</sup> through toll-like receptor-mediated signaling pathways and the subsequent transcriptional inhibition of inflammatory genes.<sup>34</sup> However, the therapeutic application of hBD3 has some limitations, including the difficulty of mass production due to its long amino acid sequence and the decreased stability observed at high ionic strength. Importantly, three disulfide bonds containing six cysteines maintain the stability of the hBD3 structure, as well as its anti-inflammatory properties.<sup>11</sup> When cysteine residues in hBD3 were substituted with serines, the induction of TNF- $\alpha$  by LPS was not inhibited, and immune reactions induced by LPS were, in fact, significantly enhanced.<sup>34</sup>

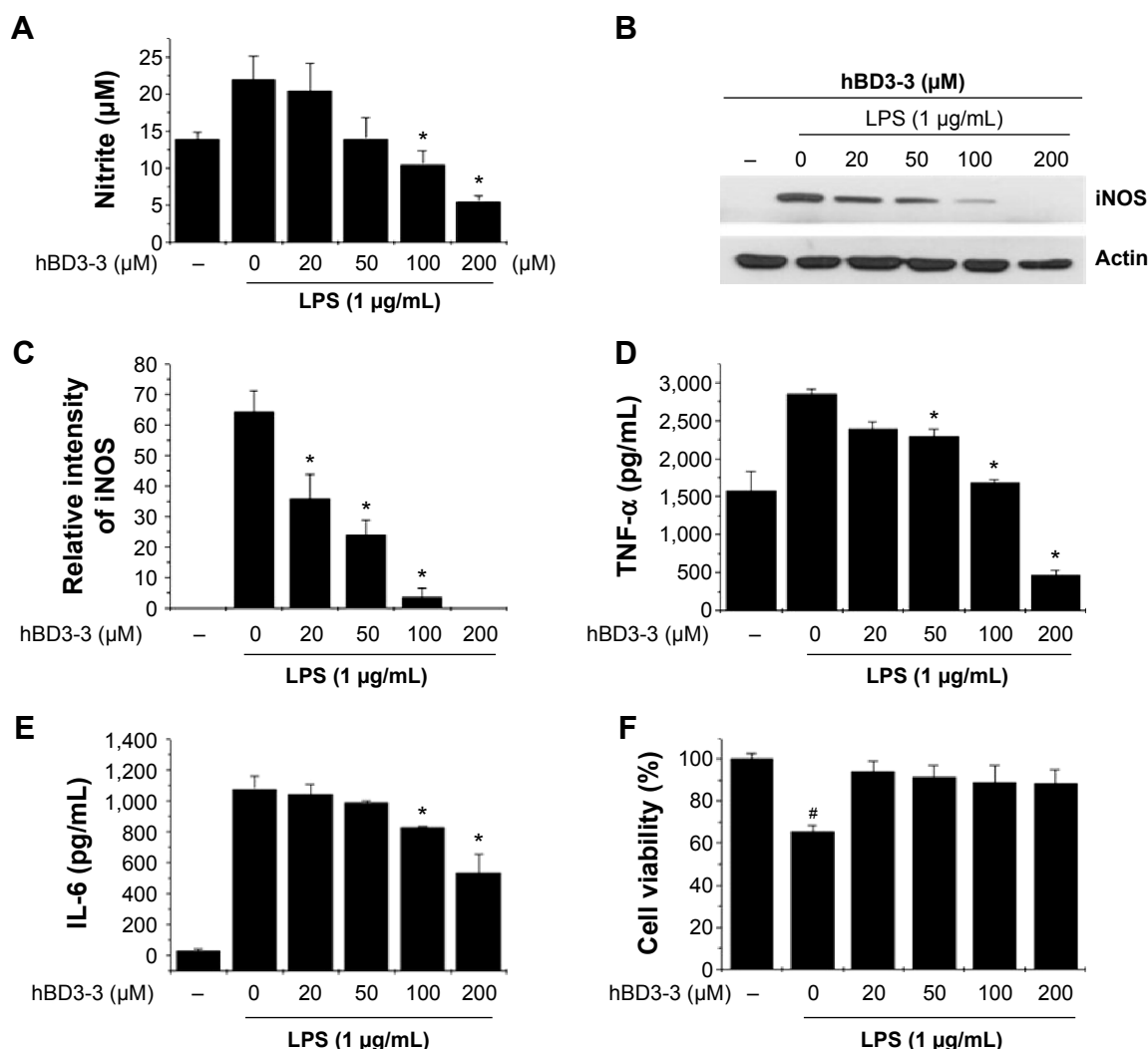


**Figure 4** The effects of hBD3-3 on LPS-induced NO, iNOS, and cytokine production in RAW 264.7 cells.

**Notes:** Cells were treated with the indicated concentrations of hBD3 for 1 hour before the addition of LPS (1 μg/mL) for 18 hours. Unstimulated cells were used as controls. (A) Quantitative analysis of NO production. Equal amounts of total protein (40 μg) were subjected to 10% SDS-PAGE. (B) The expression of the iNOS and actin proteins was detected through Western blot analysis using specific antibodies. (C) The level of iNOS was normalized to that of actin. Quantitative analysis of (D) TNF-α and (E) IL-6 production. (F) Cytotoxicity of hBD3-3 in RAW 264.7 cells. Cells were incubated with various concentrations of hBD3-3 for 24 hours. The number of viable cells remaining in the wells was assessed using the 3-(4,5-dimethylthiazol-2-yl)-2,5-diphenyltetrazolium bromide assay and compared with untreated cells. The data are expressed as the mean ± SD from three independent experiments in each group. \**P* < 0.05 versus the 1 μg/mL LPS-treated group. #*P* < 0.05 versus the untreated control group.

**Abbreviations:** hBD3, human beta-defensin 3; LPS, lipopolysaccharide; NO, nitric oxide; iNOS, inducible nitric oxide synthase; SDS-PAGE, sodium dodecyl sulphate-polyacrylamide gel electrophoresis; TNF-α, tumor necrosis factor-α; IL-6, interleukin-6; SD, standard deviation; MTT, 3-(4,5-dimethylthiazol-2-yl)-2,5-diphenyltetrazolium bromide.

Recently, various functional peptides have been investigated that might replace the effect of impermeable molecules that play an essential role in the biochemical and physiological competences of the human body.<sup>35</sup> Unlike other β-defensins, the high positive charge (note: the net charge is +11) of hBD3 may contribute to its broad-spectrum microbial eradicating ability by binding directly to microbial pathogens.<sup>36</sup> The purpose of this study was to isolate a key peptide fragment from hBD3 that shows both intracellular localization activity and anti-inflammatory activity. Our results indicated that all of the hBD3 fragments that we tested in the translocation analyses (Figures 1–3) were detected both in cells and in animal skin

(Figures 2 and 3). In particular, hBD3-3 showed the most significant penetration in both target cells and tissue. These results suggest that hBD3-3 may exhibit the most potent effect for delivering drugs, such as paramagnetic particles, nucleic acids, proteins, and peptides. Moreover, the observed cell-penetrating activity is an important mechanism underlying the antimicrobial and immunosuppressive effects of hBD3. However, further studies are needed to elucidate the action of cysteines in hBD3-3 that can maintain their structure or influence on anti-inflammatory responses.

Focusing on hBD3-3, we examined its anti-inflammatory mechanism as well as its penetrating activity in LPS-induced



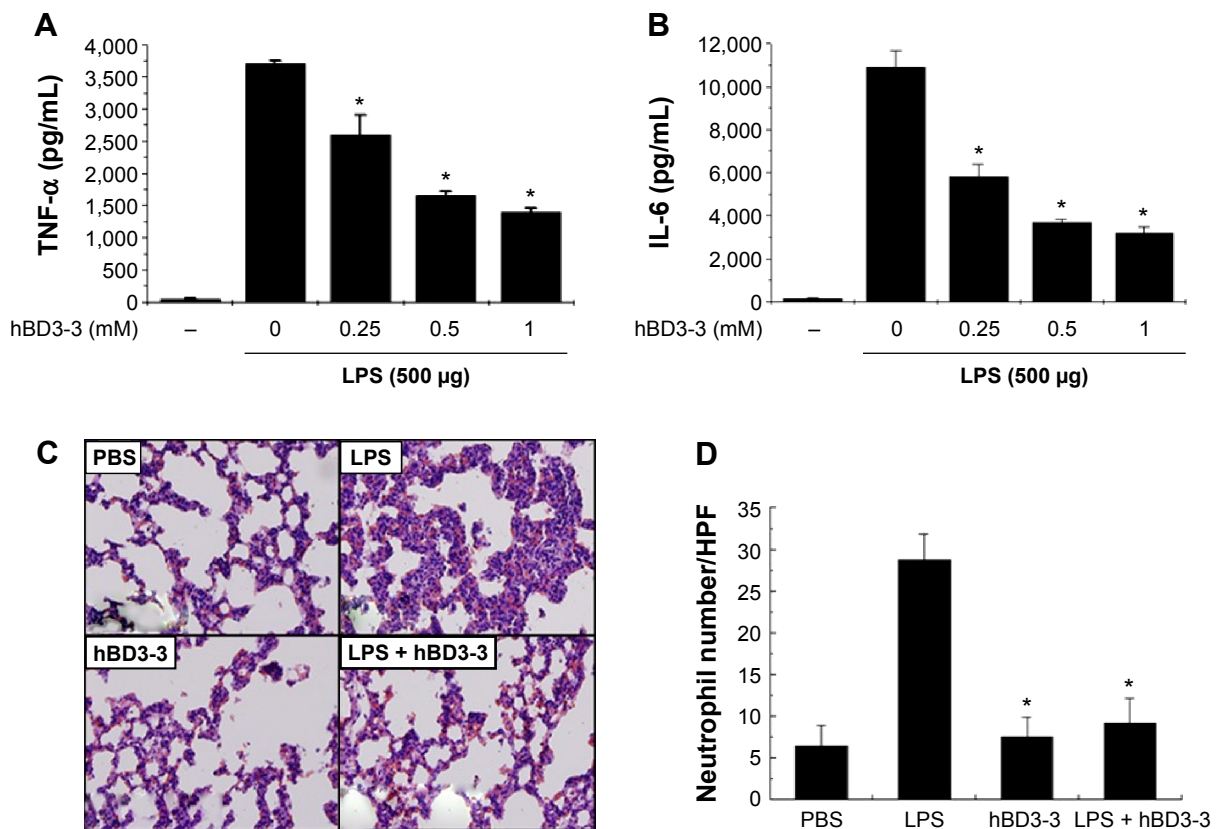


**Figure 5** Effect of hBD3-3 on LPS-induced lung inflammation in vivo.

**Notes:** Rats were treated with the indicated concentrations of hBD3-3 and 500 μg of LPS for 2 hours. Quantitative analysis of (A) TNF-α and (B) IL-6 expression in plasma. The data are expressed as the mean ± SD from three independent experiments in each group. \* $P < 0.05$  versus the 500 μg LPS-treated group. (C) Histological analysis of leukocyte infiltration in the peribronchial and interstitial areas of the lungs through H&E staining (magnification: 200×). (D) Quantitative analysis of neutrophil sequestration in the lungs. The analysis was performed using lung specimens stained with H&E. Neutrophil infiltration was expressed as the number of neutrophils per high-power field by counting the number in over 30 fields at a magnification of 400× on each slide. The data are expressed as the mean ± SD from three independent experiments in each group. \* $P < 0.05$  versus the LPS-treated group.

**Abbreviations:** hBD3, human beta-defensin 3; LPS, lipopolysaccharide; TNF-α, tumor necrosis factor-α; SD, standard deviation; IL-6, interleukin-6; H&E, hematoxylin and eosin; PBS, phosphate-buffered solution.

macrophages. hBD3-3 repressed LPS-stimulated NF-κB activation and the expression of cytokines by the cells (Figure 4). In addition, hBD3-3 potentially inhibited LPS-induced neutrophil migration in lungs injured by inflammatory responses (Figure 5). In general, lung inflammation animal model induced by LPS to investigate an effect of anti-microbial drugs in vivo. The concentration of LPS treatment was different depending on injection method, body weight, and species of animal. Approximately 2.5–7.5 mg/kg of LPS was injected intravenously in rats.<sup>37–39</sup> We had intravenously applied the 4.1 mg/kg of LPS (body weight of ~120 g, 5–6-weeks-old Wistar rat) as an inflammatory inducer to rats in accordance with previous studies. It could induce acute lung injury that looks like pneumonia. The author investigated the effective concentration of the peptide through activity profiling containing toxicity and anti-inflammatory activity in vitro as well as in vivo.<sup>40</sup> LPS is a potent proinflammatory stimulant and exerts its effects via NF-κB activation, which

is related to the expression of many genes related to inflammatory reactions.<sup>41</sup> Thus, NF-κB is an emerging target for the treatment of inflammatory diseases.<sup>42</sup> In the unstimulated state, due to inactivation by IκBα, NF-κB remains in the cytoplasm instead of translocating to the nucleus. However, after exposure to a stimuli, such as LPS, IκBα phosphorylation increases, which triggers its proteolytic degradation, leading to NF-κB activation and the expression of genes that play important roles in innate and adaptive immunity.<sup>43,44</sup> Interestingly, hBD3-3 blocks phosphorylation-induced IκBα degradation, thereby inhibiting the nuclear migration of NF-κB p65 subunits (Figure 6). Based on these results, we suggest that hBD3-3 possesses outstanding anti-inflammatory activity through its targeting of canonical NF-κB pathway-mediated inflammation in cells. Our findings suggest new therapeutic strategies that may combat various infections in human body, as well as inflammatory diseases, such as psoriasis, atherosclerosis, pulmonary inflammation-associated disease, and

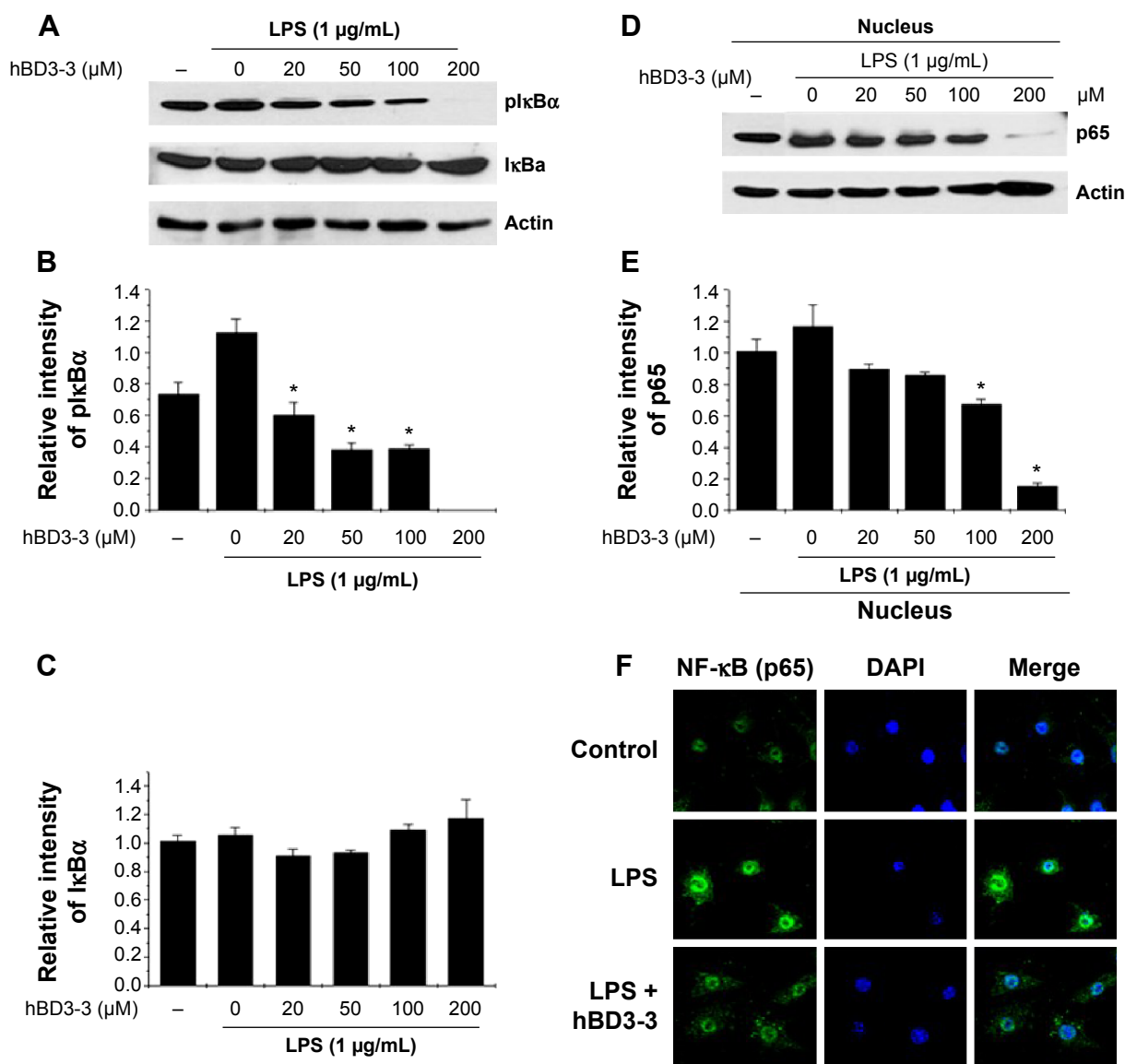


**Figure 6** Effect of hBD3-3 on LPS-induced IκBα phosphorylation and p65 nuclear translocation in RAW 264.7 cells.

**Notes:** RAW 264.7 cells were treated with the indicated concentration of hBD3-3 for 1 hour and stimulated with LPS (1 μg/mL) for 30 minutes at 37°C. (A) Western blot analysis using an anti-phospho-IκBα, anti-total IκBα, or anti-actin antibody. (B) Relative pIκBα and (C) total IκBα levels were quantified via densitometry and normalized to actin. The effect of hBD3-3 on the LPS-induced translocation of p65 subunits in RAW 264.7 cells. (D) Nuclear extracts were prepared and analyzed via Western blot analysis using anti-p65 or anti-actin antibodies. (E) Relative p65 subunit levels were quantified via densitometry and normalized to actin levels. The data are expressed as the mean ± SD from three independent experiments in each group. \**P* < 0.05 versus the 1 μg/mL LPS-treated groups. (F) RAW 264.7 cells were treated with 50 μM hBD3-3 for 1 hour and stimulated with LPS (1 μg/mL) for 30 minutes at 37°C. Fixed cells were stained with DAPI, an anti-NF-κB p65 antibody and a fluorescein isothiocyanate-conjugated anti-rabbit IgG antibody. Images were obtained via confocal microscopy.

**Abbreviations:** hBD3, human beta-defensin 3; LPS, lipopolysaccharide; SD, standard deviation; DAPI, 4',6-diamidino-2-phenylindole; NF-κB, nuclear factor-kappa B; IgG, immunoglobulin G.

arthritis.<sup>45</sup> Therefore, further studies are required to clarify the availability and the effectiveness of hBD3-3 in vivo.

## Conclusion

hBD3-3 can penetrate into cells and through mouse skin and exert anti-inflammatory action both in vitro and in vivo. The peptide suppressed NF-κB activation by directly blocking IκBα degradation (Figure 7). Based on these investigations, hBD3-3 may prove an effective pharmaceutical tool

for treating inflammatory diseases and targeting intracellular infections via its eukaryotic internalization ability. The results of our animal study support further research on hBD3-3 and its application to rheumatoid arthritis as a skin-based approach.

## Acknowledgments

This research was supported by the Bio and Medical Technology Development Program of the National Research

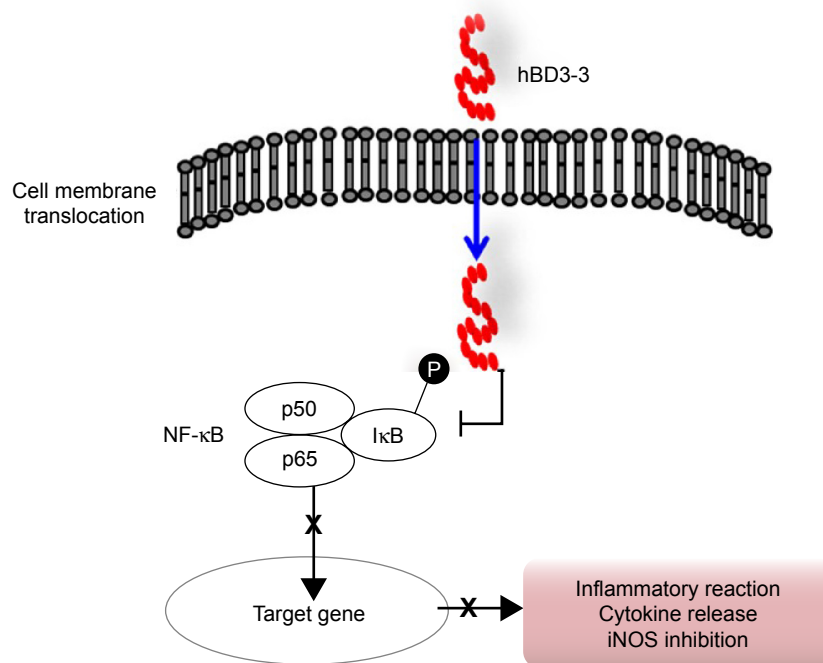


**Figure 7** The anti-inflammatory mechanism of hBD3-3 involves serial inhibition of IκBα phosphorylation, p65 nuclear translocation and, finally, NF-κB-dependent inflammatory responses in vitro and in vivo.

**Abbreviations:** hBD3, human beta-defensin 3; NF-κB, nuclear factor-kappa B; iNOS, inducible nitric oxide synthase.

Foundation (NRF) funded by the Ministry of Science, ICT and Future Planning (NRF-2014M3A9E3064431 and NRF-2014M3A9E3064433) and a grant of the Korean Health Technology R&D Project through the Korea Health Industry Development Institute (KHIDI) funded by the Ministry of Health & Welfare (HI1C1211).

## Disclosure

The authors report no conflicts of interest in this work.

## References

- Lehrer RI, Ganz T. Antimicrobial peptides in mammalian and insect host defence. *Curr Opin Immunol*. 1999;11(1):23–27.
- Guani-Guerra E, Santos-Mendoza T, Lugo-Reyes SO, Teran LM. Antimicrobial peptides: general overview and clinical implications in human health and disease. *Clin Immunol*. 2010;135(1):1–11.
- Bulet P, Stocklin R, Menin L. Anti-microbial peptides: from invertebrates to vertebrates. *Immunol Rev*. 2004;198:169–184.
- Lai Y, Gallo RL. AMPed up immunity: how antimicrobial peptides have multiple roles in immune defense. *Trends Immunol*. 2009;30(3):131–141.
- Bals R. Epithelial antimicrobial peptides in host defense against infection. *Respir Res*. 2000;1(3):141–150.
- Selsted ME, Ouellette AJ. Mammalian defensins in the antimicrobial immune response. *Nat Immunol*. 2005;6(6):551–557.
- Harder J, Bartels J, Christophers E, Schroder JM. Isolation and characterization of human beta-defensin-3, a novel human inducible peptide antibiotic. *J Biol Chem*. 2001;276(8):5707–5713.
- Ouhara K, Komatsuzawa H, Yamada S, et al. Susceptibilities of periodontopathogenic and cariogenic bacteria to antibacterial peptides, {beta}-defensins and LL37, produced by human epithelial cells. *J Antimicrob Chemother*. 2005;55(6):888–896.
- Hoover DM, Wu Z, Tucker K, Lu W, Lubkowski J. Antimicrobial characterization of human beta-defensin 3 derivatives. *Antimicrob Agents Chemother*. 2003;47(9):2804–2809.
- Kluver E, Schulz-Maronde S, Scheid S, Meyer B, Forssmann WG, Adermann K. Structure-activity relation of human beta-defensin 3: influence of disulfide bonds and cysteine substitution on antimicrobial activity and cytotoxicity. *Biochemistry*. 2005;44(28):9804–9816.
- Wu Z, Hoover DM, Yang D, et al. Engineering disulfide bridges to dissect antimicrobial and chemotactic activities of human beta-defensin 3. *Proc Natl Acad Sci U S A*. 2003;100(15):8880–8885.
- Rivera-Monroy Z, Bonn GK, Guttman A. Fluorescent isotope-coded affinity tag 2: peptide labeling and affinity capture. *Electrophoresis*. 2009;30(7):1111–1118.
- Richard JP, Melikov K, Vives E, et al. Cell-penetrating peptides. A reevaluation of the mechanism of cellular uptake. *J Biol Chem*. 2003;278(1):585–590.
- Bae YS, Yi HJ, Lee HY, et al. Differential activation of formyl peptide receptor-like 1 by peptide ligands. *J Immunol*. 2003;171(12):6807–6813.
- Guevara I, Iwanejko J, Dembinska-Kiec A, et al. Determination of nitrite/nitrate in human biological material by the simple Griess reaction. *Clin Chim Acta*. 1998;274(2):177–188.
- Schwarze SR, Dowdy SF. In vivo protein transduction: intracellular delivery of biologically active proteins, compounds and DNA. *Trends Pharmacol Sci*. 2000;21(2):45–48.
- Schmidt N, Mishra A, Lai GH, Wong GCL. Arginine-rich cell-penetrating peptides. *FEBS Lett*. 2010;584(9):1806–1813.
- Hung CF, Lu KC, Cheng TL, et al. A novel siRNA validation system for functional screening and identification of effective RNAi probes in mammalian cells. *Biochem Biophys Res Commun*. 2006;346(3):707–720.
- Desai P, Patlolla RR, Singh M. Interaction of nanoparticles and cell-penetrating peptides with skin for transdermal drug delivery. *Mol Membr Biol*. 2010;27(7):247–259.
- Patlolla RR, Desai PR, Belay K, Singh MS. Translocation of cell penetrating peptide engrafted nanoparticles across skin layers. *Biomaterials*. 2010;31(21):5598–5607.

21. Lappas M, Permezel M, Georgiou HM, Rice GE. Nuclear factor kappa B regulation of proinflammatory cytokines in human gestational tissues in vitro. *Biol Reprod*. 2002;67(2):668–673.
22. Baueerle PA, Baltimore D. NF-kappa B: ten years after. *Cell*. 1996;87(1):13–20.
23. Jeon KI, Xu X, Aizawa T, et al. Vinpocetine inhibits NF-kappaB-dependent inflammation via an IKK-dependent but PDE-independent mechanism. *Proc Natl Acad Sci U S A*. 2010;107(21):9795–9800.
24. Dhople V, Krukemeyer A, Ramamoorthy A. The human beta-defensin-3, an antibacterial peptide with multiple biological functions. *Biochim Biophys Acta*. 2006;1758(9):1499–1512.
25. Fujii G, Selsted ME, Eisenberg D. Defensins promote fusion and lysis of negatively charged membranes. *Protein Sci*. 1993;2(8):1301–1312.
26. Wimley WC, Selsted ME, White SH. Interactions between human defensins and lipid bilayers – evidence for formation of multimeric pores. *Protein Sci*. 1994;3(9):1362–1373.
27. Niyonsaba F, Ushio H, Nakano N, et al. Antimicrobial peptides human beta-defensins stimulate epidermal keratinocyte migration, proliferation and production of proinflammatory cytokines and chemokines. *J Invest Dermatol*. 2007;127(3):594–604.
28. Biragyn A, Ruffini PA, Leifer CA, et al. Toll-like receptor 4-dependent activation of dendritic cells by beta-defensin 2. *Science*. 2002;298(5595):1025–1029.
29. Mosser DM, Zhang X. Activation of murine macrophages. *Curr Protoc Immunol*. 2008;Chapter 14:Unit 14.12.
30. Fengyang L, Yunhe F, Bo L, et al. Stevioside suppressed inflammatory cytokine secretion by downregulation of NF-kappaB and MAPK signaling pathways in LPS-stimulated RAW264.7 cells. *Inflammation*. 2012;35(5):1669–1675.
31. Jung HW, Chung YS, Kim YS, Park YK. Celastrol inhibits production of nitric oxide and proinflammatory cytokines through MAPK signal transduction and NF-kappaB in LPS-stimulated BV-2 microglial cells. *Exp Mol Med*. 2007;39(6):715–721.
32. Han JM, Jin YY, Kim HY, Park KH, Lee WS, Jeong TS. Lavandulyl flavonoids from *Sophora flavescens* suppress lipopolysaccharide-induced activation of nuclear factor-kappaB and mitogen-activated protein kinases in RAW264.7 cells. *Biol Pharm Bull*. 2010;33(6):1019–1023.
33. Semple F, Webb S, Li HN, et al. Human beta-defensin 3 has immunosuppressive activity in vitro and in vivo. *Eur J Immunol*. 2010;40(4):1073–1078.
34. Semple F, MacPherson H, Webb S, et al. Human beta-defensin 3 affects the activity of pro-inflammatory pathways associated with MyD88 and TRIF. *Eur J Immunol*. 2011;41(11):3291–3300.
35. Ganz T. Defensins: antimicrobial peptides of innate immunity. *Nat Rev Immunol*. 2003;3(9):710–720.
36. Pingel LC, Kohlgraf KG, Hansen CJ, et al. Human beta-defensin 3 binds to hemagglutinin B (rHagB), a non-fimbrial adhesin from *Porphyromonas gingivalis*, and attenuates a pro-inflammatory cytokine response. *Immunol Cell Biol*. 2008;86(8):643–649.
37. Hagiwara S, Iwasaka H, Hasegawa A, et al. Filtration leukocytapheresis therapy ameliorates lipopolysaccharide-induced systemic inflammation in a rat model. *J Surg Res*. 2011;171(2):777–782.
38. Inoue K, Takano H, Sakurai M, et al. Pulmonary exposure to diesel exhaust particles enhances coagulatory disturbance with endothelial damage and systemic inflammation related to lung inflammation. *Exp Biol Med (Maywood)*. 2006;231(10):1626–1632.
39. Liu S, Feng G, Wang GL, Liu GJ. p38MAPK inhibition attenuates LPS-induced acute lung injury involvement of NF-kappaB pathway. *Eur J Pharmacol*. 2008;584(1):159–165.
40. Lee JY, Seo YN, Park HJ, Park YJ, Chung CP. The cell-penetrating peptide domain from human heparin-binding epidermal growth factor-like growth factor (HB-EGF) has anti-inflammatory activity in vitro and in vivo. *Biochem Biophys Res Commun*. 2012;419(4):597–604.
41. Xu X, Yin P, Wan C, et al. Punicalagin inhibits inflammation in LPS-induced RAW264.7 macrophages via the suppression of TLR4-mediated MAPKs and NF-kappaB activation. *Inflammation*. 2014;37(3):956–965.
42. Kim JK, Park GM. Indirubin-3-monoxime exhibits anti-inflammatory properties by down-regulating NF-kappaB and JNK signaling pathways in lipopolysaccharide-treated RAW 264.7 cells. *Inflamm Res*. 2012;61(4):319–325.
43. Wang CC, Choy CS, Liu YH, et al. Protective effect of dried safflower petal aqueous extract and its main constituent, carthamus yellow, against lipopolysaccharide-induced inflammation in RAW 264.7 macrophages. *J Sci Food Agric*. 2011;91(2):218–225.
44. Bi WY, Fu BD, Shen HQ, et al. Sulfated derivative of 20(S)-ginsenoside Rh2 inhibits inflammatory cytokines through MAPKs and NF-kappaB pathways in LPS-induced RAW264.7 macrophages. *Inflammation*. 2012;35(5):1659–1668.
45. Gaur U, Aggarwal BB. Regulation of proliferation, survival and apoptosis by members of the TNF superfamily. *Biochem Pharmacol*. 2003;66(8):1403–1408.

## International Journal of Nanomedicine

### Publish your work in this journal

The International Journal of Nanomedicine is an international, peer-reviewed journal focusing on the application of nanotechnology in diagnostics, therapeutics, and drug delivery systems throughout the biomedical field. This journal is indexed on PubMed Central, MedLine, CAS, SciSearch®, Current Contents®/Clinical Medicine,

Submit your manuscript here: <http://www.dovepress.com/international-journal-of-nanomedicine-journal>

Dovepress

Journal Citation Reports/Science Edition, EMBASE, Scopus and the Elsevier Bibliographic databases. The manuscript management system is completely online and includes a very quick and fair peer-review system, which is all easy to use. Visit <http://www.dovepress.com/testimonials.php> to read real quotes from published authors.